# Photoemission linewidths and quasiparticle lifetimes

N. V. Smith
*AT&T Bell Laboratories, Murray Hill, New Jersey 07974*

P. Thiry and Y. Petroff*
*Laboratoire pour l'Utilisation du Rayonnement Electromagnétique, Université de Paris–Sud, F-91405 Orsay, France*

(Received 3 September 1992)

Expressions are derived for the relationship between the measured linewidths in angle-resolved valence-band photoemission spectra and the lifetimes of the photoelectron and photohole. The expressions are different for the energy-distribution curve (EDC), constant initial-state spectrum (CIS), and constant final-state spectrum modes of data acquisition, and are significantly angle dependent for the EDC and CIS. The circumstances in which the lifetime widths of the photoelectron and photohole can be separated from each other are discussed with special reference to a debate on high-temperature superconductors. Surface states offer the only case where the photohole lifetime can be rigorously isolated. The nearly-free-electron approximation is elaborated and used to explain some counterintuitive behavior in recent data on Ag(100).

## I. INTRODUCTION

The relationship between linewidths in valence-band photoemission spectra and the lifetimes of the photoelectron and photohole has been considered by a number of workers.[1–12] The aim of this paper is to offer a more comprehensive derivation of this relationship than that which has appeared in the literature so far. We shall consider the cases of both normal and off-normal emission, and we shall do it for the three principal modes of photoemission data taking [the energy-distribution curve (EDC), the constant initial-state spectrum (CIS), and the constant final-state spectrum (CFS)].

This work was stimulated by a recent discussion of photoemission linewidths on approaching the Fermi edge in high-temperature superconductors.[13–15] It emerged from the discussion that there was a need for further study of photoemission linewidths and quasiparticle lifetimes in normal materials.[16] We shall discuss below the rather restrictive circumstances in which the lifetime widths for the photoelectron ($\Gamma_f$) and the photohole ($\Gamma_i$) can be isolated from each other. In general, the expression for the measured linewidth ($\Gamma_m$) is a linear combination of $\Gamma_f$ and $\Gamma_i$ whose coefficients depend on details of the band structure, are angle dependent, and are different for the three modes of data taking. The nearly free-electron approximation will be presented and used to show how counterintuitive behavior (peaks increasing in width on approaching the Fermi edge) can occur.

Our approach is at the simplest level. It adopts narrow Lorentzian line shapes and a first-order expansion within a one-electron band structure. While we shall be considering the energy dependences of $\Gamma_i$ and $\Gamma_f$, we shall treat these parameters as constant within a spectral line. In more rigorous approaches,[1,8,12] $\Gamma_i$ and $\Gamma_f$ are the imaginary parts of the photohole and photoelectron self-energies and depend upon both energy $E$ and momentum $k$. The respective real parts of the self-energy will (through Kramers-Krönig relations) also be dependent on $E$ and $k$. Such refinements are ignored here. Indeed, the intent of this paper is to show that the extraction of quasiparticle lifetimes is potentially intricate even in the simplest of models. While our emphasis is on the intrinsic limitations of linewidth analysis, we shall discuss briefly the extrinsic (i.e., experimental) limitations, particularly the problems associated with lack of sample perfection.

## II. OPTICAL CROSS SECTION

The effects of the surface and the finite lifetimes of the photoelectron and photohole may be simulated by treating the perpendicular component of the wave vector as complex, $k_\perp = k_\perp^R + ik_\perp^I$. At this level of approximation, the cross section for an optical transition between an initial state in band $i$ and a final state in band $f$ has Lorentzian form:

$$\sigma \propto \frac{1}{(k_{i\perp}^R - k_{f\perp}^R)^2 + (k_{i\perp}^I + k_{f\perp}^I)^2} \ . \tag{1}$$

This can be derived directly from the one-step formalism of photoemission[7] or thought of as the $k_\perp$ convolution of two Lorentzians.[8,12] The cross section is maximum when $k_{i\perp}^R - k_{f\perp}^R = 0$, that is to say when the maximum of the $k_\perp$ envelope of the final state coincides with that of the initial state. This is the residue of the direct (i.e., vertical) transition selection rule. The parallel component $k_\parallel$, on the other hand, is strictly conserved. The half maximum intensity occurs when

$$k_{i\perp}^R - k_{f\perp}^R = \pm(k_{i\perp}^I + k_{f\perp}^I) \ . \tag{2}$$

This condition, which arises from the additivity of Lorentzian linewidths, is illustrated in Fig. 1 for the three principal modes of photoemission data acquisition. If $\Gamma_i$

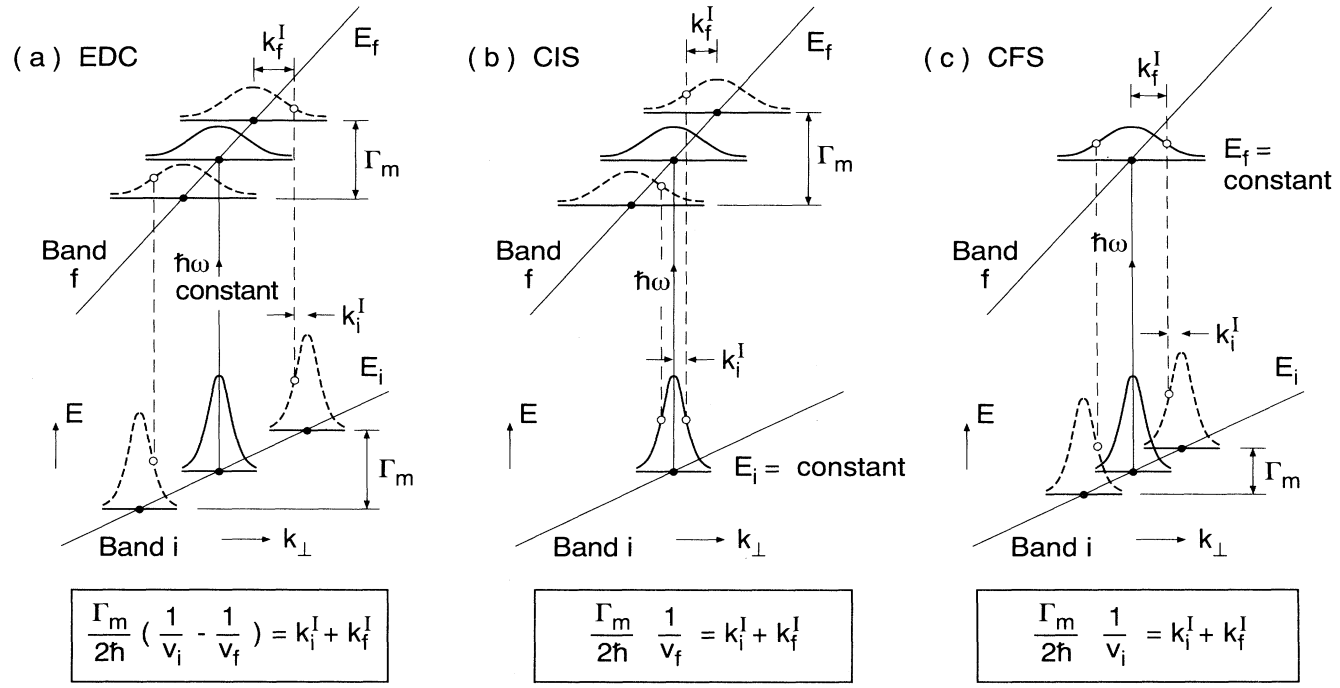


FIG. 1. Geometrical representation of the $k_\perp$-space convolution in the derivation of optical cross sections and measured linewidths ($\Gamma_m$) for the three principal modes of photoemission data taking (a) EDC (energy-distribution curve), (b) CIS (constant initial-state spectrum), and (c) CFS (constant final-state spectrum). The half-widths $k_i^I$ and $k_f^I$ are the imaginary parts of the perpendicular wave vector and are given by $\Gamma_i/2\hbar|v_i|$ and $\Gamma_f/2\hbar|v_f|$, respectively, where $\Gamma_i$ and $\Gamma_f$ are the lifetime widths of the photohole and photoelectron, and $v_i$ and $v_f$ are the respective group velocities. From the additivity of Lorentzian linewidths, the intensity at half maximum occurs when the half maximum of the final state lies directly above that of the initial state as indicted by the open circles and vertical dashed lines. (The expressions in the boxes refer to the case of normal emission.)

and $\Gamma_f$ denote the lifetime widths of the photohole (initial state) and photoelectron (final state), respectively, we have

$$k_{i\perp}^I=\Gamma_i/2\hbar|v_{i\perp}| , \tag{3}$$

$$k_{f\perp}^I=\Gamma_f/2\hbar|v_{f\perp}| , \tag{4}$$

where $v_{i\perp}$ and $v_{f\perp}$ are group velocities ($\hbar v_{i\perp}=\partial E_i/\partial k_\perp$, and so forth).

Some authors draw a physical distinction between the contributions of the photoelectron and the photohole to the spectral linewidth, emphasizing momentum broadening for the former and energy broadening for the latter.[1,12] Here, the photoelectron and photohole are treated on an equal footing. Each is held to have a well-defined energy, and the scattering effects are treated in terms of momentum broadening. A more significant physical distinction, as far as this paper is concerned, is the choice of spectrum-measurement mode.

## III. LINEWIDTH ANALYSIS

There are three principal modes of photoemission spectroscopy. The most common is the EDC mode in which the photon energy $\hbar\omega$ and the polar angle of emission $\theta$ are held constant and the spectrum is acquired by sweeping the kinetic energy $E$ of the photoelectrons. The CIS and CFS modes exploit the continuum nature of synchrotron radiation,[17] and will be defined below.

In all three modes, the following three kinematical conditions must apply. First, energy conservation requires

$$\delta E_f-\delta E_i-\delta\hbar\omega=0 . \tag{5}$$

Second, conservation of parallel momentum ($k_{f\|}-k_{i\|}=g_\|$, where $\mathbf{g}$ is a reciprocal lattice vector) requires

$$\delta k_{f\|}=\delta k_{i\|}=\delta k_\| . \tag{6}$$

Third, the kinetic energy $E$ ($\equiv E_f-E_V$, where $E_V$ is the vacuum level) of the photoelectron in vacuum is given by $\hbar^2k_\|^2/2m\sin^2\theta$, where

$$\delta E_f=-\frac{\hbar^2k_\|^2\cos\theta}{m\sin^3\theta}\delta\theta+\frac{\hbar^2k_\|}{m\sin^2\theta}\delta k_\| . \tag{7}$$

In all three modes, $\theta$ is held strictly constant ($\delta\theta=0$), so we may write

$$\delta k_\|=\frac{m\sin^2\theta}{\hbar^2k_\|}\delta E_f . \tag{8}$$

In addition to these kinematical constraints, we have, by definition of the group velocities for the real bands

$E_f(k_{f\parallel},k_{f\perp}^R)$ and $E_i(k_{i\parallel},k_{i\perp}^R)$,

$$\delta E_f=\hbar v_{f\perp}\delta k_{f\perp}^R+\hbar v_{f\parallel}\delta k_{f\parallel}\ , \tag{9}$$

$$\delta E_i=\hbar v_{i\perp}\delta k_{i\perp}^R+\hbar v_{i\parallel}\delta k_{i\parallel}\ . \tag{10}$$

Our procedure is to examine the consequences of Eqs. (9) and (10) for the different measurement modes. We shall assume perfect instrumental resolution in both energy and angle section. That is to say we concentrate on the *intrinsic* broadening mechanisms associated with the photoelectron and photohole lifetimes. (A brief discussion of *extrinsic* broadening mechanisms is offered below in Sec. IV D.)

### A. EDC mode

In the EDC mode, $\hbar\omega$ is held constant ($\delta\hbar\omega=0$) so that $\delta E_i=\delta E_f=\delta E$. Invoking Eqs. (6) and (8), Eqs. (9) and (10) become

$$\hbar v_{f\perp}\delta k_{f\perp}^R=\left[1-\frac{mv_{f\parallel}\sin^2\theta}{\hbar k_{\parallel}}\right]\delta E\ , \tag{11}$$

$$\hbar v_{i\perp}\delta k_{i\perp}^R=\left[1-\frac{mv_{i\parallel}\sin^2\theta}{\hbar k_{\parallel}}\right]\delta E\ . \tag{12}$$

Let us introduce $k_{0\perp}^R$ as that perpendicular wave vector for which the cross section is maximum. The left-hand side of Eq. (2) becomes

$$k_{i\perp}^R-k_{f\perp}^R=(k_{i\perp}^R-k_{0\perp}^R)-(k_{f\perp}^R-k_{0\perp}^R)=\delta k_{i\perp}^R-\delta k_{f\perp}^R\ . \tag{13}$$

Thus from Eq. (2), the half maximum intensity condition is

$$\begin{aligned}\frac{\delta E}{\hbar}&\left[\frac{1}{v_{i\perp}}\left[1-\frac{mv_{i\parallel}\sin^2\theta}{\hbar k_{\parallel}}\right]-\frac{1}{v_{f\perp}}\left[1-\frac{mv_{f\parallel}\sin^2\theta}{\hbar k_{\parallel}}\right]\right]\\&=\pm(k_{i\perp}^I+k_{f\perp}^I)\\&=\pm(\Gamma_i/2\hbar|v_{i\perp}|+\Gamma_f/2\hbar|v_{f\perp}|)\ .\end{aligned} \tag{14}$$

Finally, noting that $\Gamma_m=2|\delta E|$, we obtain

$$\Gamma_m=\frac{\Gamma_i/|v_{i\perp}|+\Gamma_f/|v_{f\perp}|}{\left|\frac{1}{v_{i\perp}}\left[1-\frac{mv_{i\parallel}\sin^2\theta}{\hbar k_{\parallel}}\right]-\frac{1}{v_{f\perp}}\left[1-\frac{mv_{f\parallel}\sin^2\theta}{\hbar k_{\parallel}}\right]\right|}\ . \tag{15}$$

This derivation has been presented previously by Thiry.[7] The $\sin^2\theta$ terms have the following physical interpretation. Holding $\theta$ constant while sweeping $E$ means that $k_{\parallel}$ is varying across the width of the spectral line. Depending on the magnitudes and signs of $v_{i\parallel}$ and $v_{f\parallel}$, this can compress or expand the measured linewidth. Equation (15) has been quoted also by Chiang *et al.*,[5] but without derivation. The appearance of $\theta$-dependent terms has been disputed by Grepstad, Slagsvold, and Bartos[8] but their treatment explicitly neglects the variation of $k_{\parallel}$ across the line.

### B. CIS mode

In the CIS mode, $E_i$ is held constant, and the spectrum is acquired by sweeping the kinetic energy $E$ ($\equiv E_f-E_V$) and $\hbar\omega$ synchronously. We have $\delta E_i=0$, and so $\delta E_f=\delta\hbar\omega=\delta E$. Equations (9) and (10) become

$$\hbar v_{f\perp}\delta k_{f\perp}^R=\left[1-\frac{mv_{f\parallel}\sin^2\theta}{\hbar k_{\parallel}}\right]\delta E\ , \tag{16}$$

$$\hbar v_{i\perp}\delta k_{i\perp}^R=\left[0-\frac{mv_{i\parallel}\sin^2\theta}{\hbar k_{\parallel}}\right]\delta E\ . \tag{17}$$

Noting that $\Gamma_m=2|\delta E|$, we obtain

$$\Gamma_m=\frac{\Gamma_i/|v_{i\perp}|+\Gamma_f/|v_{f\perp}|}{\left|-\frac{1}{v_{i\perp}}\left[\frac{mv_{i\parallel}\sin^2\theta}{\hbar k_{\parallel}}\right]-\frac{1}{v_{f\perp}}\left[1-\frac{mv_{f\parallel}\sin^2\theta}{\hbar k_{\parallel}}\right]\right|}\ . \tag{18}$$

As in the EDC, $k_{\parallel}$ can vary across a spectral line, and this can compress or expand the measured linewidth.

### C. CFS mode

In the CFS mode, $E_f$ is held constant, and the spectrum is acquired by sweeping $\hbar\omega$. We have $\delta E_f=\delta E=0$, and so $\delta\hbar\omega=-\delta E_i$. Also $\delta k_{f\parallel}=\delta k_{i\parallel}=\delta k_{\parallel}=0$. Equations (9) and (10) become

$$\hbar v_{f\perp}\delta k_{f\perp}^R=0\ , \tag{19}$$

$$\hbar v_{i\perp}\delta k_{i\perp}^R=-\delta\hbar\omega\ . \tag{20}$$

Noting that $\Gamma_m=2|\delta\hbar\omega|$, we obtain

$$\Gamma_m=\frac{\Gamma_i|v_{i\perp}|+\Gamma_f/|v_{f\perp}|}{1/|v_{i\perp}|}\ . \tag{21}$$

In the CFS, $E$ and $\theta$ are constant. There is therefore no variation of $k_{\parallel}$ across the spectral line, and therefore no $\theta$-dependent terms in $\Gamma_m$. This strong difference in the $\theta$ dependence of the EDC, CIS, and CFS modes is the principal new result of this paper, and could form the basis of an experimental strategy to test linewidth analysis. (A similar set of results can be obtained for inverse photoemission by a trivial reversal of the definitions of initial and final states.)

## IV. LIMITING CASES

### A. Normal emission

In the case of normal emission ($\theta=0$), the measured linewidths are given by

$$\text{EDC:}\quad \Gamma_m\left|\frac{1}{v_{i\perp}}-\frac{1}{v_{f\perp}}\right|=\frac{\Gamma_i}{|v_{i\perp}|}+\frac{\Gamma_f}{|v_{f\perp}|}\ , \tag{22}$$

$$\text{CIS:}\quad \Gamma_m\left|\frac{1}{v_{f\perp}}\right|=\frac{\Gamma_i}{|v_{i\perp}|}+\frac{\Gamma_f}{|v_{f\perp}|}\ , \tag{23}$$

$$\text{CFS:}\quad \Gamma_m\left|\frac{1}{v_{i\perp}}\right|=\frac{\Gamma_i}{|v_{i\perp}|}+\frac{\Gamma_f}{|v_{f\perp}|}\ . \tag{24}$$

These expressions are identical with those in the boxes of Figs. 1(a), 1(b), and 1(c). The normal emission expression

for the EDC is the expression usually quoted in the literature. Note, however, that even for normal emission the expressions for the EDC, CIS, and CFS are significantly different from each other.

### B. Isolation of $\Gamma_f$

If the initial states are sufficiently close to the Fermi level $E_f$, we have $\Gamma_i \to 0$, and the linewidths are then totally determined by the photoelectron lifetime parameter $\Gamma_f$. A particularly simple case is offered by the CIS. If $\Gamma_i$ can be neglected, we may equate $\Gamma_m$ with $\Gamma_f$. This identity has been asserted, without derivation, by Eastman and co-workers,[2,3] and their results are shown in Fig. 2. In normal emission EDC's from Cu(100), there is a direct-transition peak which crosses $E_F$ in the photon energy range $\hbar\omega = 9-12$ eV. The open squares in Fig. 2 represent the intensity in the EDC just below the Fermi edge ($E_i = E_F - 0.13$ eV). This is a CIS, albeit taken point-by-point rather than by a continuous sweep of $\hbar\omega$. The data points fall close to a Lorentzian curve whose full at half maximum (FWHM) can be equated with $\Gamma_f$ (1.2 eV in this particular case). An analogous situation arises in inverse photoemission with those instruments which employ parallel detection over $\hbar\omega$, as opposed to the more conventional isochromat mode.

### C. Isolation of $\Gamma_i$

Another useful limit occurs when $|v_{i\perp}|$ is much smaller than the other group velocities, that is to say, when the energy dispersion of the initial-state band perpendicular to the surface is very small. The normal emission cases for both the EDC and CFS give

$$\Gamma_m = \Gamma_i + \left| \frac{v_{i\perp}}{v_{f\perp}} \right| \Gamma_f \ . \tag{25}$$

In the extreme case when $v_{i\perp}$ vanishes (i.e., a perfectly flat band perpendicular to the surface), we may identify $\Gamma_m$ with $\Gamma_i$, the imaginary part of the photohole self-energy. This identity is sometimes tacitly assumed, particularly in recent discussions on high-temperature superconductors.

An excellent example here is the linewidth analysis performed by Knapp, Himpsel, and Eastman[3] on normal emission EDC's within the $d$ band of Cu. The $d$ bands are rather flat, and their $E(k)$ dispersion is well known. The dispersion of the final-state bands is also well established. It is therefore possible to make a confident estimate of the magnitude of the second term in Eq. (25); it turns out to be $\sim 0.1$ eV, considerably smaller than the measured linewidths (0.3–0.6 eV) permitting a reliable correction to $\Gamma_m$ and the isolation of $\Gamma_i$. Very similar analyses have been presented in Ref. 7.

Layer compounds furnish a class of materials in which $v_{i\perp}$ is small. The high-temperature superconducting materials are also good candidates. $Bi_2Sr_2CaCu_2O_8$ is especially interesting since it can be cleaved in vacuum and generates very-high-quality angle-resolved photoemission spectra.[13] Much interest has focused on the finding that $\Gamma_m$ varies linearly on approaching $E_F$, and this is regarded as possible evidence of non-Fermi-liquid-like behavior.[14,15] Some actual values of $v_{i\perp}$ are known from the band calculations of Mattheiss[18] and are illustrated in Fig. 3, which shows the $k$-space average values $\langle v_{i\perp} \rangle$ calculated for $Bi_2Sr_2CaCu_2O_8$. At $E_F$, $\langle v_{i\perp} \rangle \sim 0.04 \times 10^8$ cm/sec, and this leads to an estimate of 30–50 meV for the second term in Eq. (25). This may help to explain the nonzero intercept at $E = E_F$.[16] Moreover, the $\langle v_{i\perp} \rangle$ curve has strong structure showing a peak just below $E_F$. Structure in the nonaveraged $v_{i\perp}$ for the specific $k$ directions investigated experimentally could be even stronger, and will distort attempts to isolate the energy dependence of $\Gamma_i$. On the other hand, it can be argued that the electronic structure of these materials is so anomalous that band theory is of limited applicability.[14,19] Specifically, since this material is essentially insulating in the perpen-

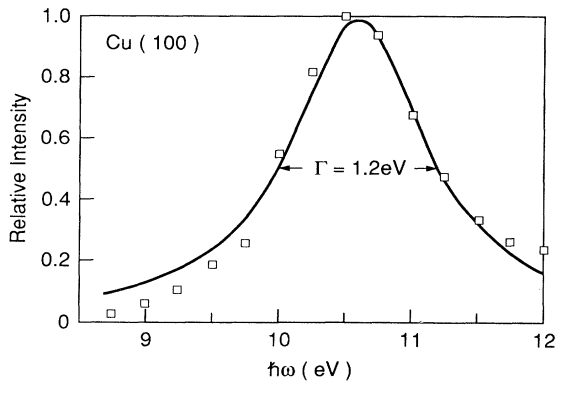


FIG. 2. CIS intensity (open squares) for a direct transition in Cu(100) with initial energy held at $E_i = E_F - 0.13$ eV. The $\hbar\omega$ dependence can be simulated quite well with a Lorentzian. Since we may take $\Gamma_i = 0$, the width 1.2 eV can be equated directly with $\Gamma_f$ [from Knapp, Himpsel, and Eastman (Ref. 3)].

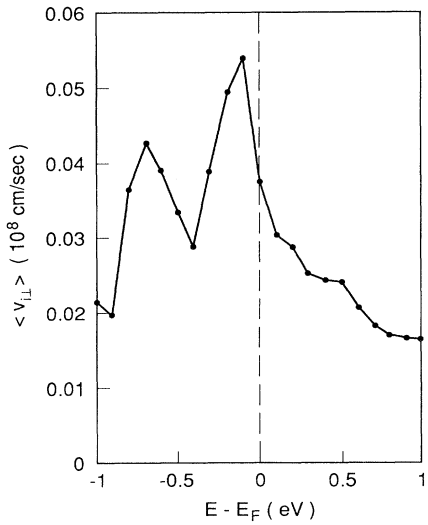


FIG. 3. Averaged perpendicular group velocity $\langle v_{i\perp} \rangle$ for $Bi_2Sr_2CaCu_2O_8$ as a function of $E_i$ as generated in a first-principles one-electron band calculation by Mattheiss (Ref. 18).

dicular direction, band calculations such as those in Fig. 3 can be expected to overestimate $v_{i\perp}$.

In principle, a rigorous isolation of $\Gamma_i$ can be achieved by measuring photoemission from *surface states*. Such states have no dispersion with $k_\perp$, and so we have $v_\perp=0$ and $\Gamma_m=\Gamma_i$. An attempt to realize this condition was made some years ago by Kevan[20] using a well-known surface state at the center of the surface Brillouin zone on Cu(111). The intent was to demonstrate that $\Gamma_m$ decreased as $E_i\rightarrow E_F$. The actual measurements showed that $\Gamma_m$ increased. This surprising result has been attributed to an extrinsic broadening mechanism which will be discussed immediately below.

### D. Extrinsic broadening mechanisms

Tersoff and Kevan[21] have rationalized the anomalous results on Cu(111) by invoking some sort of in-plane scattering from surface defects or impurity atoms. The surface state in question disperses parabolically ($E=\hbar^2k_\parallel^2/2m^*$, with $m^*=0.4m$) and crosses $E_F$ at $k_\parallel=0.2$ Å$^{-1}$. A constant mean free path $l$ would imply a constant $\Delta k_\parallel$ smearing and an increasing $\Delta E$ smearing on approaching $E_F$. The actual results imply a value $l\sim$ 30 Å, which is plausibly consistent with surface defects or impurities at the $\sim 1\%$ level.

The importance of inhomogeneous broadening associated with surface imperfection has recently received dramatic confirmation in high-resolution angle-resolved photoemission experiments by Hricovini *et al.*[22] on "ideally hydrogen terminated" Si(111) surfaces. The hydrogen terminated surfaces yield much sharper spectra than untreated Si(111) surfaces, and the clear conclusion is that a high degree of assured surface perfection is required if narrow intrinsic linewidths are to be observed.

Surface states still remain the best hope for observing $\Gamma_i\rightarrow 0$, because this is the only case for which $v_{i\perp}$ vanishes exactly. In support of this statement, we note that the sharpest structure seen in angle-resolved photoemission so far is the $\overline{M}$ Tamm state on Cu(001) reported by Wincott *et al.*[23] This feature has FWHM of 28 meV at $T\sim 150$ K, a result which is quite remarkable since this feature originates from almost 2 eV below $E_F$.

Finally, we reemphasize that our analysis has assumed perfect instrumental energy resolution and angle resolution. The effect of finite angular resolution on linewidth determination is treated in detail in Ref. 7. Such corrections must, of course, be considered in any attempt to monitor $\Gamma_i$ as $E_i\rightarrow E_F$.

## V. NEARLY-FREE-ELECTRON APPROXIMATION

### A. Linewidth expressions

It is instructive to examine linewidth expressions for the simplest of band structures, the free-electron or nearly-free-electron model. The band energies $E_i$ and $E_f$ are given by $\hbar^2k^2/2m$ and $\hbar^2(\mathbf{g}-\mathbf{k})^2/2m$, respectively. Let us take the case where the reciprocal lattice vector $\mathbf{g}$ is perpendicular to the surface. It is then easy to show that

$$mv_{i\perp}=\hbar k_\perp=-(\hbar g/2)(1-\hbar\omega/E_g)\ , \tag{26}$$

$$mv_{f\perp}=\hbar(g-k_\perp)=(\hbar g/2)(1+\hbar\omega/E_g)\ , \tag{27}$$

where $E_g=\hbar^2g^2/2m$. Since $mv_{i\parallel}=mv_{f\parallel}=\hbar k_\parallel$, Eqs. (15), (18), and (21) reduce to

$$\Gamma_m=\frac{1+\hbar\omega/E_g}{2\cos^2\theta}\Gamma_i+\frac{1-\hbar\omega/E_g}{2\cos^2\theta}\Gamma_f\ , \tag{28}$$

$$\Gamma_m=\frac{1+\hbar\omega/E_g}{\cos 2\theta-\hbar\omega/E_g}\Gamma_i+\frac{1-\hbar\omega/E_g}{\cos 2\theta-\hbar\omega/E_g}\Gamma_f\ , \tag{29}$$

$$\Gamma_m=\Gamma_i+\frac{1-\hbar\omega/E_g}{1+\hbar\omega/E_g}\Gamma_f\ . \tag{30}$$

for the EDC, CIS, and CFS, respectively. These expressions display once again the strong differences for the EDC, CIS, and CFS modes and also the strong differences in their angular dependence.

### B. Example: Ag(001) EDC's

Hwu *et al.*[24] have recently published a linewidth analysis of experimental EDC measurements of a bulk band-structure feature on Ag(001) as $E_i\rightarrow E_F$. Their results for $\Gamma_m$ (full width at half maximum) are shown as the open circles in Fig. 4. At first sight, the data look anomalous since $\Gamma_i\rightarrow 0$ as $E_i\rightarrow E_F$, whereas $\Gamma_m$ is actually *increasing* as $E_i\rightarrow E_f$. The resolution of this apparent anomaly lies in the fact that for a *bulk* transition such as this, $\Gamma_m$ is dominated by $\Gamma_f$ rather than $\Gamma_i$. Putting this more quantitatively, Eq. (28) becomes, for the conditions of this experiment ($\hbar\omega=14$ eV, $E_g=36$ eV),

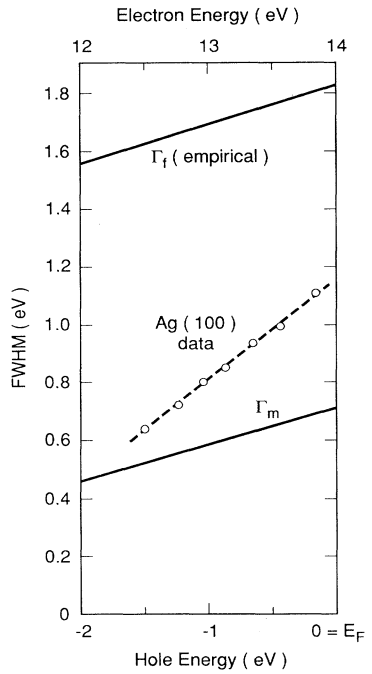


FIG. 4. Experimental EDC linewidths from Ref. 24 (open circles) taken on Ag(100) are compared with $\Gamma_m$ predicted by the nearly-free-electron model taking $\Gamma_i=0$ and using an empirical $\Gamma_f$ curve (Ref. 25).

$$\Gamma_m \sim (0.31)\Gamma_f/\cos^2\theta \ . \quad (31)$$

$\Gamma_f$ is expected to increase over the energy range of the experimental data. A recent analysis for a number of similar metals[25] suggests $\Gamma_f = 0.13(E_f - E_F)$, and this relation is shown in Fig. 4. The derived values for $\Gamma_m$ are also shown in Fig. 4. There are two main points of agreement with experiment. First, the measured values $\Gamma_m$ are lower than the empirical $\Gamma_f$ by about a factor of 3. This large demagnification is a consequence of the large group-velocity ratio. Second, the predicted $\Gamma_m$ increases as $E_i \rightarrow E_F$. About half of this increase is due to the increase of $\Gamma_f$, and the other half is due to the $\cos^2\theta$ term in the denominator of Eq. (31). The residual quantitative discrepancy is attributed to the approximations of the model and to the uncertainties in subtraction of a background before the line fitting of the experimental spectra. Extrinsic effects associated with finite instrumental resolution may also contribute.

## VI. CONCLUDING REMARKS

This paper offers a strategy for future studies of photoemission linewidths in normal materials. The strong differences in the expressions for the EDC, CIS, and CFS modes, as well as the anticipated strong angular dependence of the EDC and CIS linewidths could provide a stringent test of internal consistency. The first step, however, would be to investigate whether the expressions presented here are borne out by experiment or whether a more elaborate analysis is called for. It is clear than any such investigation must be in close association with band-structure determinations since the band derivatives are needed in the separation of $\Gamma_i$ and $\Gamma_f$. The ultimate goal is to refine the analysis to the point where we can address the behavior of the photohole lifetime on approaching close to the Fermi level.

*Present address: European Synchrotron Radiation Facility, F-38043 Grenoble, France.

[1]J. B. Pendry, in *Photoemission and the Electronic Properties of Surfaces,* edited by B. Feuerbacher, B. Fitton, and R. F. Willis (Wiley, New York, 1978), p. 87.
[2]D. E. Eastman, J. A. Knapp, and F. J. Himpsel, Phys. Rev. Lett. **41**, 825 (1978).
[3]J. A. Knapp, F. J. Himpsel, and D. E. Eastman, Phys. Rev. B **19**, 4952 (1979).
[4]P. Thiry, D. Chandresis, J. Lecante, C. Guillot, R. Pinchaux, and Y. Petroff, Phys. Rev. Lett. **43**, 82 (1979).
[5]T. C. Chiang, J. A. Knapp, M. Aono, and D. E. Eastman, Phys. Rev. B **21**, 3513 (1980).
[6]S. D. Kevan and D. A. Shirley, Phys. Rev. B **22**, 542 (1980).
[7]P. Thiry, thesis, Université de Paris–Sud, 1981.
[8]J. K. Grepstad, B. J. Slagsvold, and I. Bartos, J. Phys. F **12**, 1679 (1982).
[9]F. J. Himpsel, D. E. Eastman, and E. E. Koch, Phys. Rev. B **24**, 1687 (1981).
[10]H. J. Levinson, F. Greuter, and E. W. Plummer, Phys. Rev. B **27**, 727 (1983).
[11]B. J. Slagsvold, J. K. Grepstad, and P. O. Gartland, Phys. Scr. **T4**, 65 (1983).
[12]J. E. Inglesfield and E. W. Plummer, in *Angle Resolved Photoemission,* edited by S. D. Kevan (Elsevier, New York, 1992), p. 15.
[13]C. G. Olson, R. Liu, D. W. Lynch, R. S. List, A. J. Arko, B. W. Veal, Y. C. Chang, P. Z. Liang, and A. P. Paulikas, Phys. Rev. B **42**, 381 (1990).
[14]P. W. Anderson and J. R. Schrieffer, Phys. Today **44** (6), 54 (1991), and references therein.
[15]C. M. Varma, P. B. Littlewood, S. Schmitt-Rink, E. Abrahams, and A. E. Ruckenstein, Phys. Rev. Lett. **63**, 1996 (1989).
[16]N. V. Smith, Comments Condens. Matter Phys. **15**, 263 (1992).
[17]G. J. Lapeyre, A. D. Baer, J. Anderson, J. C. Hermanson, J. A. Knapp, and P. L. Gobby, Solid State Commun. **15**, 1601 (1974).
[18]L. F. Mattheiss (unpublished), quoted in Ref. 16.
[19]P. W. Anderson, Science, **235**, 1196 (1987); and private communication.
[20]S. D. Kevan, Phys. Rev. Lett. **50**, 526 (1983).
[21]J. Tersoff and S. D. Kevan, Phys. Rev. B **28**, 4267 (1983).
[22]K. Hricovini, R. Günther, P. Thiry, A. Taleb-Ibrahimi, G. Indlekofer, J. E. Bonnet, P. Dumas, Y. Petroff, X. Blase, Xuejun Zhu, Steven G. Louie, Y. J. Chabal, and P. A. Thiry, Phys. Rev. Lett. **70**, 1992 (1993).
[23]P. L. Wincott, N. B. Brookes, D. S.-L. Law, and G. Thornton, Phys. Rev. B **33**, 4373 (1986).
[24]Y. Hwu, L. Lozzi, S. La Rosa, M. Onellion, P. Almeras, F. Gozzo, F. Lévy, M. Berger, and G. Margaritondo, Phys. Rev. B **45**, 5483 (1992).
[25]A. Goldman, W. Altmann, and V. Dose, Solid State Commun. **79**, 511 (1991).